

*Tectonophysics*, 21 (1974) 15-38

© Elsevier Scientific Publishing Company, Amsterdam - Printed in The Netherlands

## THERMAL ASPECTS OF SEA-FLOOR SPREADING, AND THE NATURE OF THE SUBOCEANIC LITHOSPHERE \*

YAN BOTTINGA

*Université Paris VI, Institut de Physique du Globe de Paris, Laboratoire de Géochimie\*\**, Paris (France)

(Accepted for publication April 27, 1973)

### ABSTRACT

Bottinga, Y., 1974. Thermal aspects of sea-floor spreading, and the nature of the suboceanic lithosphere. *Tectonophysics*, 21: 15-38.

By means of a kinematic model, plate generation at the spreading center is investigated numerically. Petrological differentiation, partial melting with concomitant latent-heat effects, and convection have been taken into consideration. Geothermal gradients are calculated for the suboceanic lithosphere at various distances from the spreading center. The nature of layer 3 is discussed. It is concluded that besides a lateral mineralogical zonation, the suboceanic lithosphere should also display a vertical variation in its chemical composition.

### INTRODUCTION

In the theory of plate tectonics, the generation of the suboceanic lithosphere plays an important role. Consequently this region has recently been a focus of attention, and large amounts of data with a bearing on this subject have been published. Certain features of the ocean bottom are nearly universally accepted, such as the reality of sea-floor spreading, and the uniformity of the ocean-ridge basalts. Many authors have postulated rising currents of partially molten material underneath the crests of the oceanic rises, to fill up the void created by the spreading lithosphere. Part of the difficulty of interpreting the vast collection of data may be due to the fact, that the consequences of sea-floor spreading have not been fully realized. The oceanic lithosphere moves at speeds of about one or more centimeters per year. In regions where the upper mantle is partially molten one should anticipate buoyancy-induced differential motion between the solid and the liquid phases. Underneath the ocean rises, where upward currents of mantle material traverse considerable pressure and temperature intervals, equilibrium may not be attained when minerals tend to change their chemical composition, or undergo phase changes, as a response to varying pressure and temperature. However, the relative chemical uniformity of ocean-ridge basalts gives the impression that a steady state has been reached.

In this paper a model of the suboceanic lithosphere will be discussed, in which are in-

\* Contribution: I.P.G. N.S. 76.

\*\* Laboratoire associé CNRS LA 196.



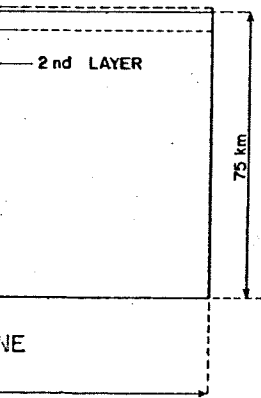
of these features are not  
 ical differentiation is allowed  
 obtain an understanding  
 or spreading.  
 ading centre. Rise and ridge  
 velocity. The region which  
 km is called the upper mantle.  
 ed otherwise. Rocknames are  
 erite is used it is meant to  
 ks with a picritic composi-  
 al.cm<sup>-2</sup>sec<sup>-1</sup>.

ERE

iven by Langseth et al.  
 model of Bottinga and

a narrow zone (Matthews

ect layers, layers 2 and 3 of  
 e top of the low-velocity



lyl.

- (4) Layer 2 of the oceanic crust consists of ocean-ridge tholeiite (Le Pichon, 1969).
- (5) The mean composition of the suboceanic lithosphere is equivalent to pyrolite (Ringwood, 1966).
- (6) The water concentration in the upper mantle is, on the average, very low (Moore, 1970).
- (7) Temperature at the top of the plate is 0°C.
- (8) Temperature at the bottom of the plate is 1350°C.

Using the data given in Appendix 2, and the conclusion of Langseth and Von Herzen (1970), and of Sclater and Francheteau (1970) that the observed heat flow in the undisturbed ocean basin, far away from spreading centers, is about 1.3 HFU one can calculate a steady-state temperature of 1350°C for the plate bottom.

DESCRIPTION OF THE MODEL

The upper mantle is thermodynamically something like a twelve-component system, and may be even worse, whose phase relationships are only known in a reconnaissance fashion. Using the Ito and Kennedy (1968) results, this complicated system has been reduced, for the purpose of this paper, to a pseudo-binary system in which basalt, pyrolite, and peridotite are intermediate compositions, see Fig.2. Compositions in this diagram are expressed as fraction basalt and fraction peridotite. The compositions more acidic than basalt have a fraction basalt greater than unity and a negative fraction peridotite; the algebraic sum of the fractions is of course equal to one. The solid-liquid phase relations in Fig.2 are completely determined by the basalt-peridotite liquidus and solidus. These curves are known for various temperatures and pressures, therefore diagrams like Fig.2 may be constructed for all pressures in the suboceanic lithosphere. The liquidus and solidus

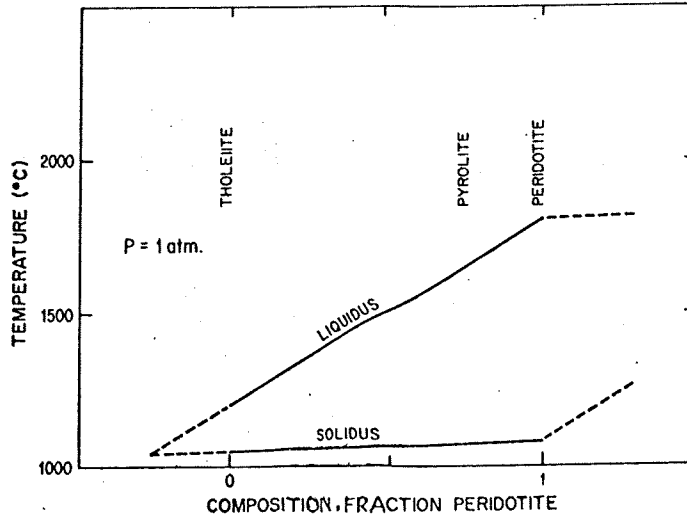


Fig.2. Assumed phase diagram, giving phase relations at 1 atm. pressure for a system in which tholeiite and peridotite are intermediate compositions.

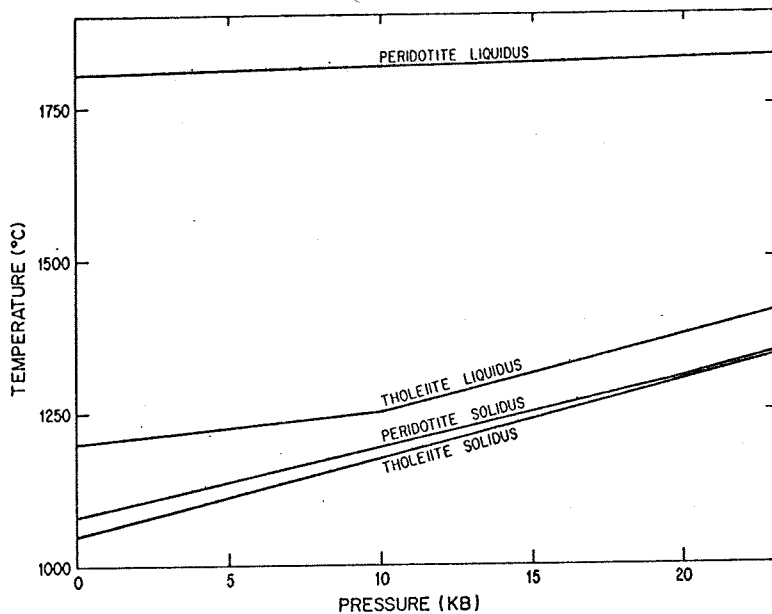


Fig. 3. Solidus and liquidus curves for tholeiite and peridotite, based upon the work by Cohen et al. (1967), and Ito and Kennedy (1967, 1968).

curves for tholeiite and peridotite which were used in the computations are given in Fig. 3, they are virtually the same as those determined by Kennedy and his coworkers (Cohen et al., 1967; Ito and Kennedy, 1967, 1968). The extent of melting is assumed to be proportional to the fraction of the melting interval which has been traversed for a given composition. The above-cited work by Kennedy and his coworkers is in fair agreement with this assumption. The proportionality is well obeyed during the solidification of Hawaiian tholeiitic lava-lakes (Peck et al., 1966; Wright and Weiblen, 1968).

Hence, when solid and liquid are present, a composition  $x$  at pressure  $P$  will have a temperature:

$$T = T_S(P, x) + [T_L(P, x) - T_S(P, x)] F \quad (1)$$

where  $T_S(P, x)$  = solidus temperature of composition  $x$  at pressure  $P$ ;  $T_L(P, x)$  = liquidus temperature; and  $F$  = fraction of melted material.

$T_S(P, x)$  can be calculated by linear interpolation or extrapolation from the solidus temperature of basalt ( $x = 0$ ) and the solidus temperature of peridotite ( $x = 1$ ) at pressure  $P$ .

$T_L(P, x)$  may be calculated in a similar fashion. The pressure variation for the basalt solidus is given by:

$$T_S(z, 0) = 1050 + 4.17z \quad (2)$$

where  $z$  is equal to depth in kilometers and the variable  $P$  has been replaced by  $z$ , assuming that the pressure is equal to the lithostatic pressure and the average density is equal to  $3.3 \text{ g/cm}^3$ . For the basalt liquidus at depth less than 30 km:

$$T_L(z, 0) = 1200 + 1.70z$$

And for depth larger than 30 km:

$$T_L(z, 0) = 1251 + 4.10(z - 30)$$

The peridotite solidus at depth less than 30 km:

$$T_S(z, 1) = 1080 + 3.77z$$

and for over 60 km:

$$T_S(z, 1) = 1306 + 4.17(z - 60)$$

The peridotite liquidus is given by:

$$T_L(z, 1) = 1806 + 0.33z$$

Eq. 2 - 7 are based on the work of Kennedy (1967); though slight modifications of  $10^\circ\text{C}$ .

These relationships are only valid for the upper mantle, but they serve as a guide, much aimed at providing quantitative data, are concerned, but to indicate the general fact that a melt in equilibrium exists holds for this model. This is particularly true for differential movements of liquids.

Energy transport in this model is achieved by using an effective thermal conductivity. Convection in this model, one of the other is differential movement (Frank, 1968). In the absence of a magma chamber at point  $(y, z)$  may be calculated.

$$\rho C_p \frac{\partial T}{\partial t} = K \left[ \frac{\partial^2 T}{\partial y^2} + \frac{\partial}{\partial z} \left( \dots \right) \right]$$

where  $\rho$  = density;  $C_p$  = specific heat;  $T$  = temperature;  $y$  = distance from the ridge center;  $z$  = vertical distance, positive is downward;  $v_y$  = horizontal velocity;  $H$  = heat production per unit mass;  $gT\alpha/C_p$ ;  $g$  = gravitational constant.

The first term at the right

$$T_L(z, 0) = 1200 + 1.70z \quad (3)$$

And for depth larger than 30 km:

$$T_L(z, 0) = 1251 + 4.10(z - 30) \quad (4)$$

The peridotite solidus at depth less than 60 km is given by:

$$T_S(z, 1) = 1080 + 3.77z \quad (5)$$

and for over 60 km:

$$T_S(z, 1) = 1306 + 4.17(z - 60) \quad (6)$$

The peridotite liquidus is given by:

$$T_L(z, 1) = 1806 + 0.33z \quad (7)$$

Eq. 2 - 7 are based on the work of Ito and Kennedy (1967, 1968), and Cohen et al. (1967); though slight modifications have been applied, which never amount to more than 10°C.

These relationships are of course inadequate to express precisely what happens in the upper mantle, but they serve here as a first approximation. Further the model is not so much aimed at providing quantitatively exact information as far as the petrological aspects are concerned, but to indicate qualitatively what one may expect to find. The experimental fact that a melt in equilibrium with an ultra-basic solid silicate is less basic than the solid holds for this model. This is really the important feature one needs in a model with differential movements of liquids and solids.

Energy transport in this model occurs by conduction and radiation, which are treated by using an effective thermal conductivity, and by convection. There are two types of convection in this model, one is bulk motion, whose velocity field is given in Fig. 1, the other is differential movement of the liquid and solid when partial melting has occurred (Frank, 1968). In the absence of a liquid phase, the variation of temperature with time at point  $(y, z)$  may be calculated from eq. 8:

$$\rho C_P \frac{\partial T}{\partial t} = K \left[ \frac{\partial^2 T}{\partial y^2} + \frac{\partial}{\partial z} \left( \frac{\partial T}{\partial z} - \frac{\partial T_a}{\partial z} \right) \right] - \rho C_P \left[ v_y \frac{\partial T}{\partial y} + v_z \left( \frac{\partial T}{\partial z} - \frac{\partial T_a}{\partial z} \right) \right] + \rho q \quad (8)$$

where  $\rho$  = density;  $C_P$  = specific heat at constant pressure;  $K$  = effective thermal conductivity;  $T$  = temperature;  $y$  = horizontal coordinate, perpendicular to the ridge, origin at the ridge center;  $z$  = vertical coordinate, originating at the ridge crest, positive direction is downward;  $v_y$  = horizontal bulk velocity;  $|v_z| = |v_y|$ ;  $v_z$  = vertical bulk velocity;  $q$  = heat production per unit mass, by radioactive decay;  $\partial T_a / \partial z$  = adiabatic gradient =  $gT\alpha/C_P$ ;  $g$  = gravitational constant; and  $\alpha$  = coefficient of thermal expansion.

The first term at the right hand side (RHS) of eq. 8 expresses energy transport by con-

Downloaded from ascelibrary.org by University of California, San Diego on 06/11/14

duction and radiation. The second term at the RHS is the convective term for the bulk motion. The last term at the RHS of eq. 8 takes into account radiogenic energy release.

The terms involving the adiabatic gradient have been discussed by Bottinga and Allegre (1973, Appendix). There are the following functional dependences in the factors used in eq. 8:  $T = T(y, z, t)$ ,  $C_p = C_p(T)$ ,  $v_y = v_y(y, z)$  and  $v_z = v_z(y, z)$ . When melting occurs, eq. 8 should be modified to incorporate latent-heat effects and energy effects and energy transport due to buoyancy-induced differential motion of the liquid and solid:

$$\begin{aligned} \rho C_p \frac{\partial T}{\partial t} = & A - \rho C_p [Fv_L + (1-F)v_S] \left( \frac{\partial T}{\partial z} - \frac{\partial T_a}{\partial z} \right) \\ & - \rho C_p \left[ F \frac{\partial v_L}{\partial z} + (1-F) \frac{\partial v_S}{\partial z} + (v_L - v_S) \frac{\partial F}{\partial z} \right] T \\ & - \rho L \frac{\partial F}{\partial t} - \rho L \left[ F \frac{\partial v_L}{\partial z} + v_y \frac{\partial F}{\partial y} + (v_z + v_L) \frac{\partial F}{\partial z} \right] \end{aligned} \quad (9)$$

where  $A$  = RHS of eq. 8;  $v_L$  = vertical velocity of the liquid phase, measured in a frame moving with velocity  $v_y$ ;  $v_S$  = idem for solid; and  $L$  = latent heat of fusion.

The velocity  $v_L$  may be estimated by means of eq. 10, which was derived by Frank (1968):

$$v_L = F^2 a^2 g (\rho_L - \rho_S) / (640 \eta) \quad (10)$$

where  $a$  = average diameter of crystals in the liquid phase;  $\rho_L$  = density of liquid phase;  $\rho_S$  = idem for solid; and  $\eta$  = viscosity of the liquid phase.

To prevent the formation of voids, the upward moving liquid current should be balanced by a downward moving solid current:

$$v_S = - \frac{\rho_L}{\rho_S} \left( \frac{F}{1-F} \right) v_L \quad (11)$$

The second and the third term at the RHS of eq. 9 represent two-phase convection. The last two terms at the RHS of eq. 9 express latent-heat effects. Utilizing eq. 1, one obtains:

$$\frac{\partial F}{\partial t} = \frac{1}{T_L - T_S} \frac{\partial T}{\partial t} \quad (12)$$

From eq. 9 and 12 one may derive an explicit expression for the temperature variation with time in a partially melted upper mantle. Eq. 8, 9 and 10 are the basis for a finite-difference scheme, according to which the temperature distribution in the upper mantle was computed, for full details see Appendix 1.

The suboceanic lithosphere is created by letting a 150 km wide column of material

rise from the LVZ underneath. Two-phase convection occurs in the upper mantle. The two-phase convection starts at the center of this current escapes gradually from the ocean bottom at the center of layer 2. Layer 3 is formed by the liquid for layer 2 has been rising convection current under the convection current has been in the suboceanic lithosphere. Movement of solid in the ridge region. Movement of lateral mineralogical inhomogeneity. Only latent-heat effects associated with layer 3 have been taken into account. Relations in the basalt - peridotite associated with solid - solid

#### LAYER 3 AND OCEANIC HEAT

In the discussion of the results that the units of the oceanic heat flow and layer 2.

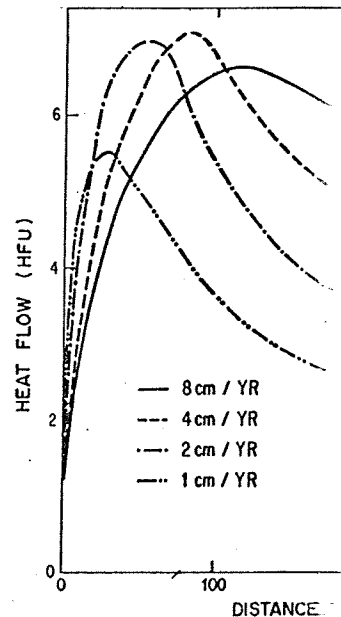


Fig. 4. Calculated heat flow. 1 HFU = 100 W/m<sup>2</sup>.

corrective term for the bulk radiogenic energy release. ... by Bottinga and Allegre ... in the factors used in ... When melting occurs, ... energy effects and energy ... liquid and solid:

(9)

... measured in a frame ... of fusion. ... was derived by Frank

(10)

... density of liquid phase; ... current should be balanced

(11)

... two-phase convection. ... Utilizing eq. 1, one

(12)

... the temperature variation ... the basis for a finite- ... in the upper mantle ... the column of material

rise from the LVZ underneath the ridge crest. The current is presumably an expression of convection occurring in the mantle. Upon rising, partial fusion takes place and subsequently two-phase convection starts (Frank, 1968). The liquid in the central 10 km wide column of this current escapes gradually at depth less than 30 km via a system of fractures to the ocean bottom at the center of the ridge. There it erupts as tholeiitic basalt and forms layer 2. Layer 3 is formed by hydration of the residual material at the ridge center after the liquid for layer 2 has been released. The partial-fusion products in other parts of the rising convection current underneath the ridge, remain in the mantle and solidify when the convection current has been deflected laterally, see Fig.1. Vertical chemical variation in the suboceanic lithosphere will be caused by the differential motion of liquid and solid in the ridge region. Moving away from the ridge, the plate cools and this will cause lateral mineralogical inhomogeneity in layer 4. In the calculations presented in this paper only latent-heat effects associated with fusion, solidification, and serpentinization of layer 3 have been taken into account, see Appendix 1. Ignorance of the subsolidus phase relations in the basalt - peridotite system prevents the incorporation of latent-heat effects associated with solid - solid transformations.

LAYER 3 AND OCEANIC HEAT FLOW

In the discussion of the results of the computations, it is for reasons of convenience that the units of the oceanic lithosphere will be discussed in the sequence layer 3, layer 4, and layer 2.

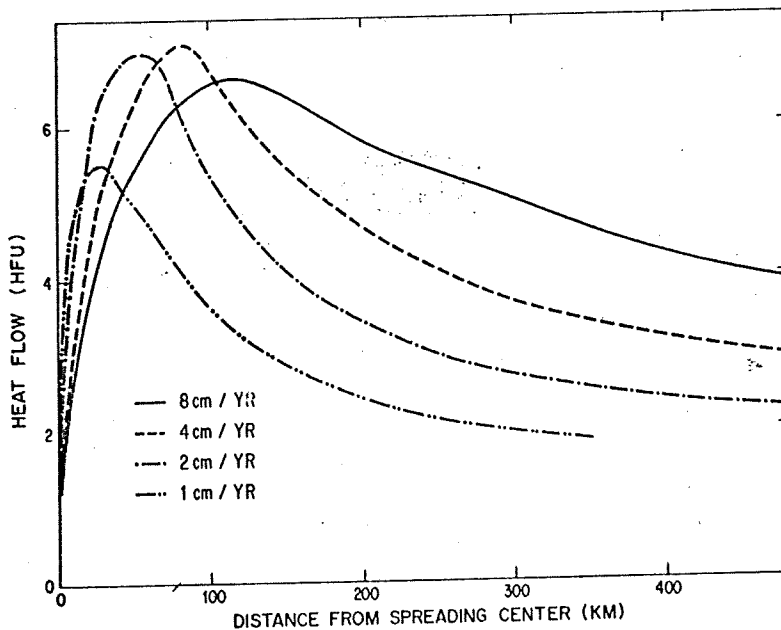


Fig.4. Calculated heat flow. 1 HFU =  $1 \cdot 10^{-6}$  cal.cm<sup>-2</sup> sec<sup>-1</sup>.

UNIVERSITY OF MICHIGAN LIBRARIES

Attention has been drawn to the fact that calculations fail to reproduce the observed heat flow close to the ridge center (Bottinga, 1972; Lister, 1972). As a possible explanation for this discrepancy it was suggested that not only layer 2 was cooled by ocean-bottom water, but also layer 3. In the calculations in this paper this possibility has been taken into account. It was assumed that fractures in layer 2 at the ridge center allow ocean-bottom water to penetrate layer 3, causing hydration and instantaneous cooling to 100°C. The hydration of rocks usually causes expansion, hence layer 3 will progressively lose its original permeability. Compaction of layer 2 will also result in a decrease of its permeability. The net effect will be that in moving away from the ridge crest ocean-water access to layer 3 diminishes greatly. The heat-flow profiles for the present model (Fig. 4) should be compared with those calculated by Bottinga and Allegre (1973), in which case layer 3 became gradually hydrated, and with the observed profiles of Horai et al. (1970), Talwani et al. (1971), Von Herzen and Simmon (1972), Lister (1972) for the vicinity of the ridge. The profiles calculated for this paper show an increased agreement with the observations. The amplitudes of the maxima of the calculated profiles are only weakly influenced by the plate velocity. This is also the case for the profiles across the Pacific, Atlantic, and Indian Ocean, compiled by Langseth and Von Herzen (1970).

In general, heat-flow calculations are quite insensitive to chemical processes in the upper mantle. The profiles calculated by Bottinga and Allegre (1973) are not distinguishable from profiles for a model similar to the present model, but without the instantaneous cooling of layer 3 at the ridge center. Likewise the replacement of a melting interval by a melting point, for the upper-mantle material, has virtually no consequences for the heat flow (Bottinga and Allegre, 1973).

In Appendix 1, it has been outlined how serpentinization of layer 3 has been incorporated in the present model. The oxygen isotopic measurements of Wenner and Taylor (1971) on serpentinite samples of the Mid-Atlantic Ridge indicate that the process occurred at a temperature less than 200°C, and that the water of hydration must have an oxygen-isotopic composition very similar to that of normal ocean water. These observations agree with the conclusions of the present model.

In the calculation of the thermal aspects of serpentinization the heats of reaction given by Kitahara and Kennedy (1967) were used. It was found that only the extent of the serpentinization depended on the actual heats of reaction; calculated heat flow was affected only in a very minor way.

#### LAYER 4, TEMPERATURE AND COMPOSITION

Before the results of the calculation are discussed, it may be useful to point out some general consequences of the model, as it was described in the previous sections. These consequences are at variance with certain aspects of the discussions by Green (1971) and Wyllie (1971).

If the water in the upper mantle is stored in amphibole, then the breakdown of this mineral may not cause the appearance of an aqueous phase, because the released water

may be stored in phlogopite. stable under the conditions of phlogopite to store the water suboceanic lithosphere are conditions in layer 4.

Seismic evidence suggests of it will be small (Anderson upper mantle cannot be much the same as the solidus for occurs, buoyancy-induced two mechanism of heat transfer. sinking solid may eventually by:

$$J = v_L FL\rho$$

Using the figures given in melting. Comparing this with of the efficiency of this mechanism degree of partial melting in much above the solidus of layer

If one supposes that tholeiite face, react extensively with rises from the LVZ its temperature at the ocean floor its temperature about 40°C. The remaining rock. Any proposed precipitation cause of the heat of crystallization

When partial melting takes the solid has a different compositionally, layer 4 will show a solid and liquid is equivalent observational evidence to support (Peck et al., 1966; Richter fraction becomes concentrated that the permeability of layer fraction collects directly under (1966) calls the "incompatible elements, and volatiles such fraction will be present inter-enriched zone there will be a elements.

To facilitate the discussion



may be stored in phlogopite. Yoder and Kushiro (1969) have shown that phlogopite is stable under the conditions one may anticipate in layer 4. One needs only about 2 wt.% phlogopite to store the water available in layer 4. Therefore, the melting relations in the suboceanic lithosphere are unlikely to be seriously affected by the low water concentrations in layer 4.

Seismic evidence suggests that if partial melting occurs in the upper mantle, the extent of it will be small (Anderson and Sammis, 1970). This means that the temperature in the upper mantle cannot be much higher than the upper-mantle solidus. This solidus is nearly the same as the solidus for oceanic tholeiite (Ito and Kennedy, 1968). If partial melting occurs, buoyancy-induced two-phase convection (Frank, 1968) will provide an additional mechanism of heat transfer. The interstitial rising liquid will eventually solidify and the sinking solid may eventually melt. Crudely, the heat flux due to this mechanism is given by:

$$J = v_L FL\rho \quad (13)$$

Using the figures given in Appendix 2, eq. 13 gives a flux of 6 HFU for 3% partial melting. Comparing this with the observed terrestrial heat flow one obtains a clear idea of the efficiency of this mechanism. Hence there is no observational evidence for a large degree of partial melting in layer 4. Therefore the temperature in layer 4 can never be much above the solidus of layer-4 material.

If one supposes that tholeiite originates in the LVZ it should, when rising to the surface, react extensively with the wall rock. The reason for this is that when the liquid rises from the LVZ its temperature must be about 1350°C, but when the tholeiite erupts at the ocean floor its temperature is about 1200°C. Adiabatic cooling will take care of about 40°C. The remaining 110° can only be disposed of by interactions with the wall rock. Any proposed precipitation of minerals during the ascent will make things worse because of the heat of crystallization which will be liberated.

When partial melting takes place in the upper mantle, the liquid in equilibrium with the solid has a different composition from the solid. Because liquid and solid move differentially, layer 4 will show a vertical chemical variation. The differential movement of the solid and liquid is equivalent to the well-known phenomenon of "filter pressing". Direct observational evidence to support this concept comes from study of Hawaiian lava lakes (Peck et al., 1966; Richter and Moore, 1966). The net result is that the low-melting fraction becomes concentrated at the cool side of the system. In this model it is supposed that the permeability of layer 3 for silicate liquids is negligible. Hence, the low-melting fraction collects directly underneath layer 3. This fraction is enriched in what Ringwood (1966) calls the "incompatible elements", such as K, Rb, Ba, Pb, Th, U, the rare-earth elements, and volatiles such as H<sub>2</sub>O, CO<sub>2</sub>, SO<sub>2</sub>, and the noble gases. This low-melting fraction will be present interstitially between much more mafic crystals. Below this enriched zone there will be a region which will be impoverished in these incompatible elements.

To facilitate the discussion of the results, the nomenclature of Table I is used. This

TABLE I  
Nomenclature

Composition in terms of basalt fraction $X$	Designation
$X \geq 0.875$	tholeiite
$0.875 > X \geq 0.625$	olivine tholeiite
$0.625 > X \geq 0.375$	picrite
$0.375 > X \geq 0.125$	pyrolite
$0.125 > X$	peridotite

usage follows Ringwood (1966), and Ito and Kennedy (1968). To avoid confusion it should be stressed that the names in Table I refer to bulk chemical compositions and not necessarily to rock types.

The calculated compositional layering in the suboceanic lithosphere is given in Fig. 5, for plate velocities of 8, 4, 2 and 1 cm/year. Compositional variation in layer 4 as a function of distance from the ridge, when layer 4 is not yet totally solid is given for the different plate velocities in Fig. 6A, 7A, 8A, and 9A. The extent of partial melting for these different cases is given in Fig. 6B, 7B, 8B, and 9B. Inspecting Fig. 5 it is obvious that under

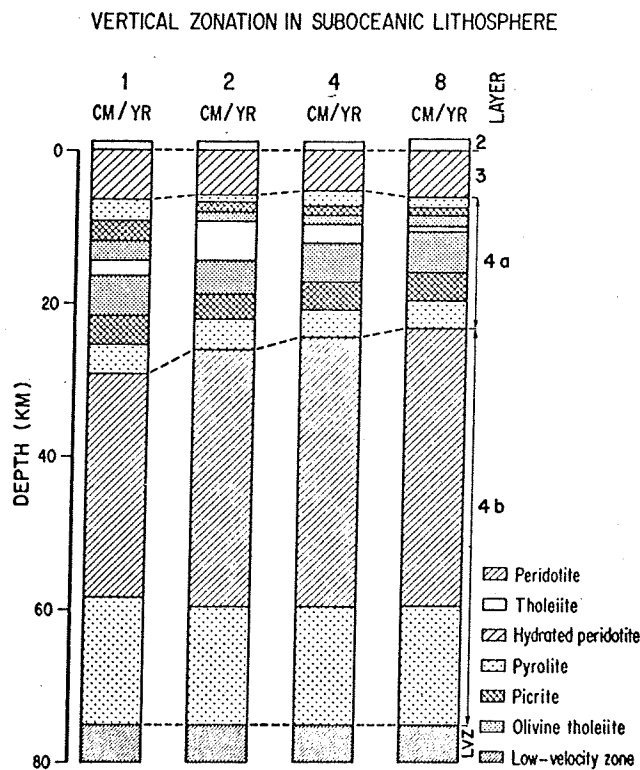


Fig. 5. Calculated steady-state compositional variations in suboceanic lithospheres moving at various plate velocities. Note rocknames refer to chemical compositions only.

To avoid confusion it  
 chemical compositions and  
 atmosphere is given in Fig.5,  
 variation in layer 4 as a func-  
 of solid is given for the differ-  
 partial melting for these  
 Fig.5 it is obvious that under

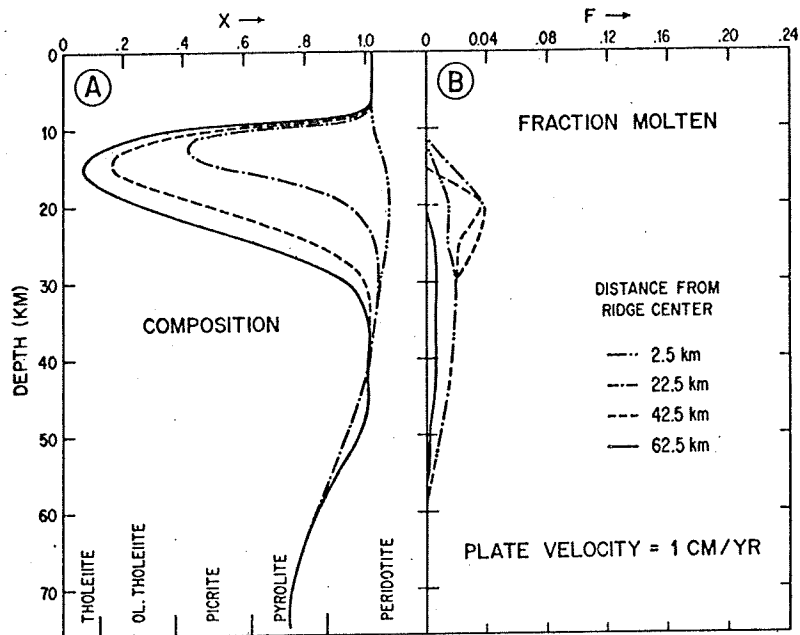


Fig.6A and B. Composition and molten fraction as they vary with depth and distance from the spreading centre, in layer 4 plate velocity = 1 cm/year.

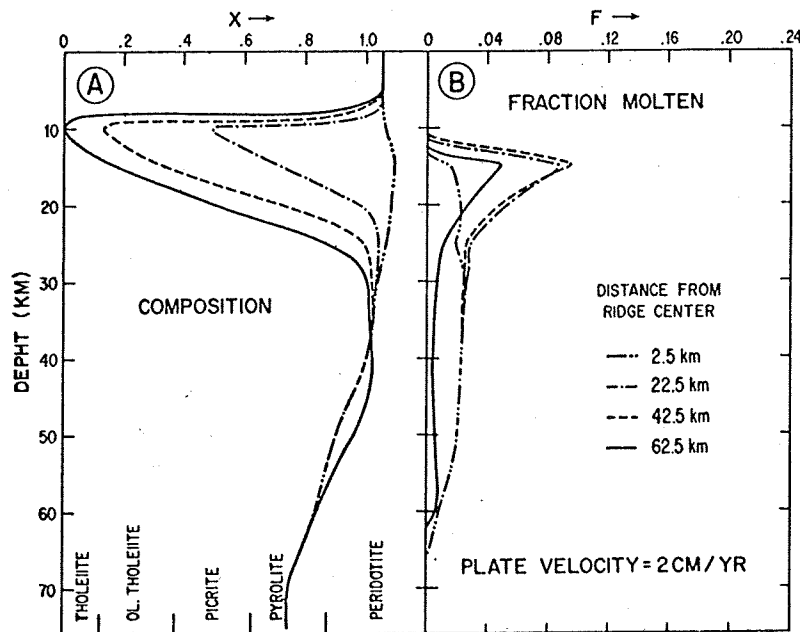


Fig.7A and B. As in Fig.6. Plate velocity = 2 cm/year.

ospheres moving at various

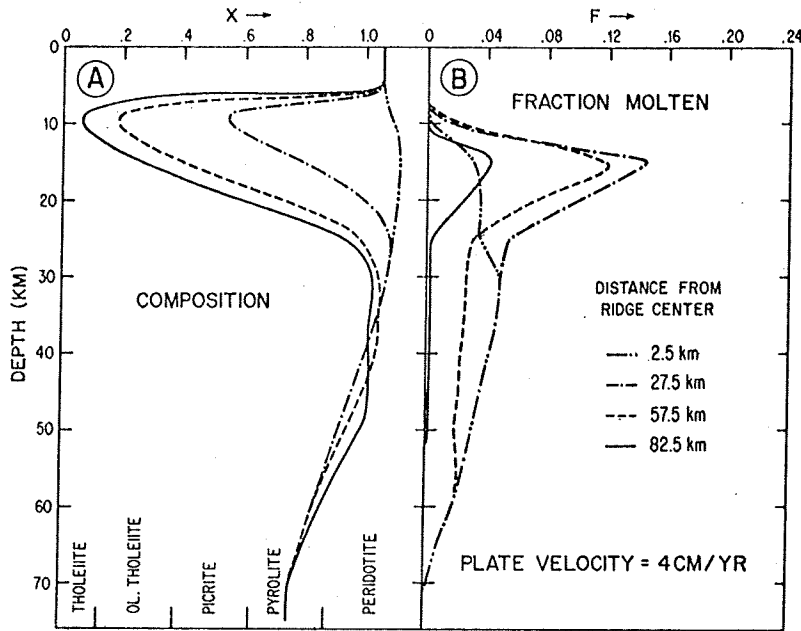


Fig. 8A and B. As in Fig. 6. Plate velocity = 4 cm/year.

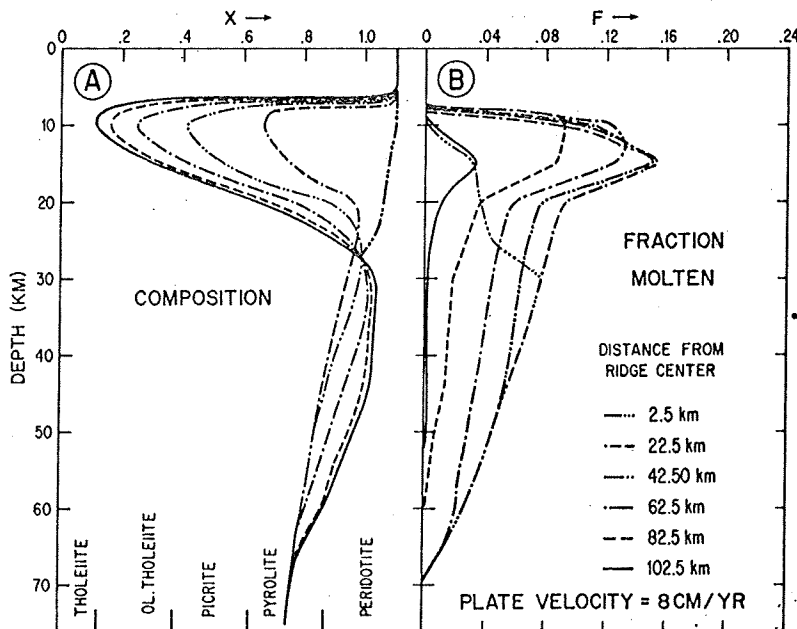


Fig. 9A and B. As in Fig. 6. Plate velocity = 8 cm/year.

## THERMAL ASPECTS OF SEA-FLOOR

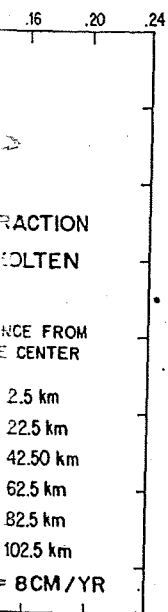
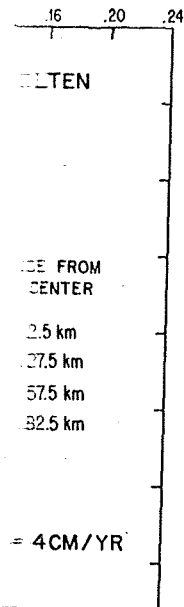
no conditions should one anticipate experienced a spreading process. In one moving at only 1 cm/year.

In all cases one may subdivide layer 4b consists of pyrolite, which is independent of the spreading rate. The extent of partial melting at the part of layer 4b consists of peridotite melting fraction, which has mixture of solid and liquid. On the other hand, by a strong vertical variation in character, layer 4a is a site of crystallization interstitially, the low melting point with depth of layer 4a depends on the thickness of layer 4a and 3.

Temperatures at various distances from the ridge center are given in Fig. 10A, 10B, 10C, and 10D. At distances greater than 100 km, the temperatures are those calculated by Bottinga and 1962. At the lithosphere temperature half the ridge center, the lowest 5 km of layer 4a is melted with depth. Above this zone, the heat is absorbed of the latent heat of crystallization.

The description by Melson and 1962 shows that there are three different mineral assemblages: a high-temperature, high-pressure assemblage (Frey, 1970); and a low-pressure assemblage consisting of talc, talc-titanite and similar minerals. Accepted as being samples of layer 4a, the samples from St. Paul's reaction, comes originally from the somewhat residual. These products form the LVZ as indicated in Fig. 11. The residual mineral assemblage between 10 and 20 km depth consists of elements, which resulted in the formation of the layer 4a. Finally, when this part of St. Paul's rocks, alteration and crystallization at temperature and -pressure assemblage.

Deuterium-hydrogen delta values for brown hornblende peridotite, and for serpentine from a partially altered sample are  $-39\%$  with respect to SMO.



no conditions should one anticipate a homogeneous suboceanic lithosphere which has experienced a spreading process. The difference between a layer 4 moving at 8 cm/year and one moving at only 1 cm/year is not great.

In all cases one may subdivide layer 4 into 4a and 4b, see Fig. 5. The lower 15 km of layer 4b consists of pyrolite, which directly overlies the LVZ. The thickness of this zone is independent of the spreading velocity. It has the same composition as the LVZ because the extent of partial melting at this depth is small, see Fig. 6B, 7B, 8B, and 9B. The top part of layer 4b consists of peridotitic material, this is essentially pyrolite minus the low-melting fraction, which has migrated upwards as a consequence of the differential movement of solid and liquid. On the top of layer 4b one finds layer 4a, which is characterized by a strong vertical variation in bulk composition. Where layer 4b has a residual, leached character, layer 4a is a site of deposition. Layer 4a is made of residual peridotite with, interstitially, the low melting fraction derived from layer 4b. The compositional variation with depth of layer 4a depends on the temperature in layer 4a and on the permeability of layer 4a and 3.

Temperatures at various distances from the centre of the ridge in layer 3 and 4 are given in Fig. 10A, 10B, 10C, and 10D, for spreading velocities of 1, 2, 4 and 8 cm/year. At distances greater than 100 km from the ridge centre these temperatures are similar to those calculated by Bottinga and Allegre (1973). At 1000 km away from the ridge centre, the lithosphere temperature has not yet attained its steady-state value. Close to the ridge centre, the lowest 5 km of layer 4 shows an almost adiabatic variation of temperature with depth. Above this zone, temperature variation with depth increases because of the absorption of the latent heat of fusion when partial melting takes place.

The description by Melson et al. (1967 and 1971) of the petrology of St. Paul's rocks shows that there are three different mineral assemblages exposed on these islets: a deformed, high-temperature, high-pressure assemblage; an undeformed intermediate-temperature and -pressure assemblage which is enriched in volatiles and incompatible elements (Frey, 1970); and a low-pressure and -temperature assemblage consisting mainly of serpentine and similar minerals. According to the present model these rocks may be interpreted as being samples of layer 4a. The high-temperature and high-pressure assemblage in the samples from St. Paul's rocks represents material, which according to this interpretation, comes originally from the LVZ, it has suffered partial melting and thus has become somewhat residual. These processes took place while the material moved upward from the LVZ as indicated in Fig. 1. Upon lateral deflection underneath the ridge crest, this residual mineral assemblage became interstitially enriched in volatiles and incompatible elements, which resulted in the intermediate-temperature and -pressure mineral assemblage. Finally, when this part of the top of layer 4 became tectonically displaced to form St. Paul's rocks, alteration and partial serpentinization took place, giving rise to the low-temperature and -pressure assemblage.

Deuterium-hydrogen delta values reported by Sheppard and Epstein (1970) for the brown hornblende peridotite, containing both primary and secondary hornblende, and for serpentine from a partially serpentinized peridotite mylonite range from  $-33$  to  $-39\%$  with respect to SMOW (Craig, 1961). The work by Arnason and Sigurgeirson

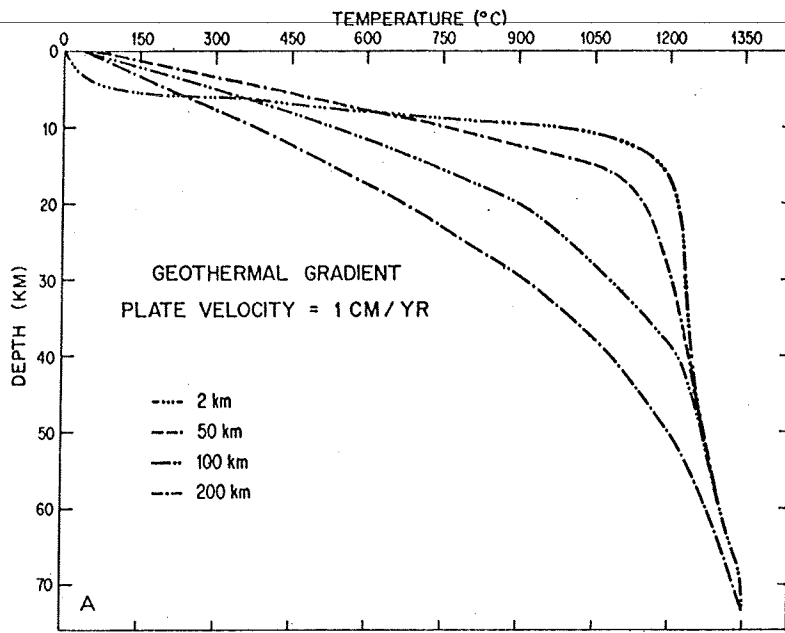


Fig.10A. Lithospheric temperatures, varying with distance from the spreading centre. Plate velocity = 1 cm/year.

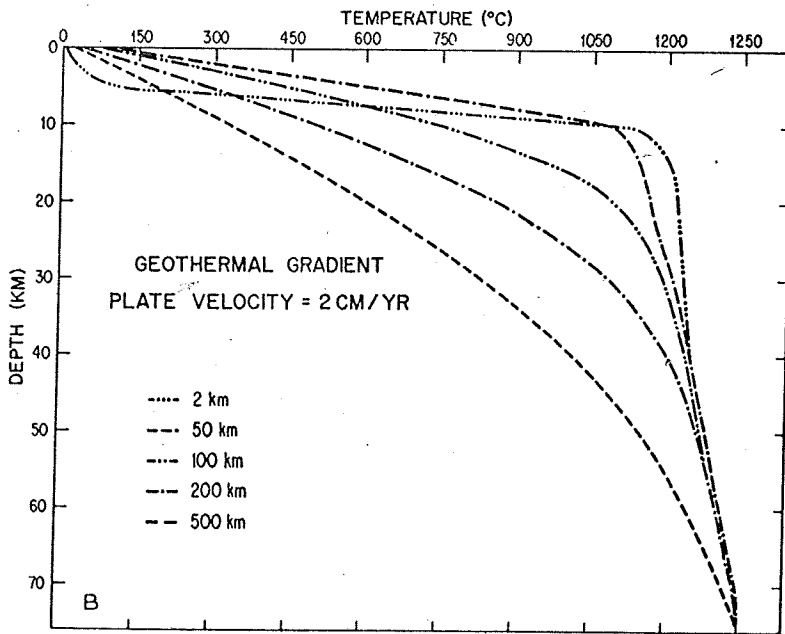


Fig.10B. As Fig.10A. Plate velocity = 2 cm/year.

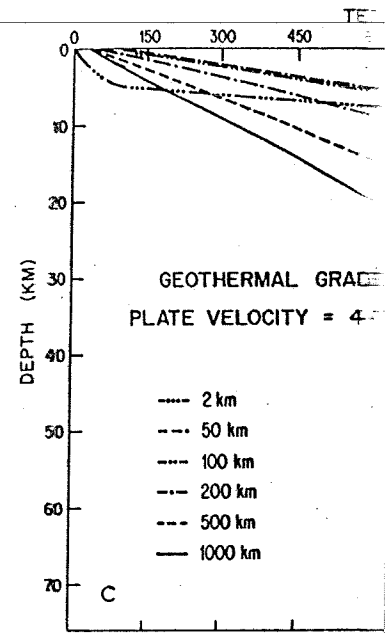


Fig.10C. As Fig.10A. Plate velocity = 4 cm/year.

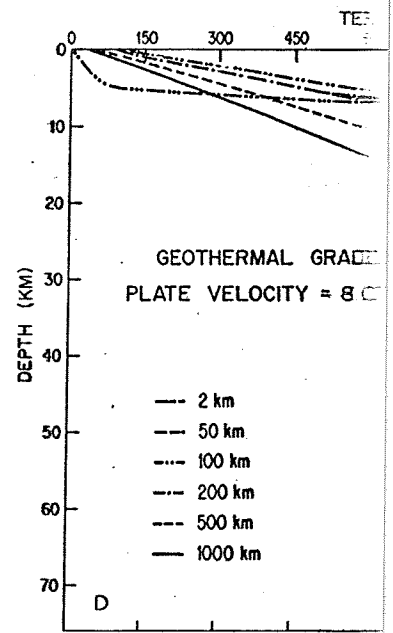
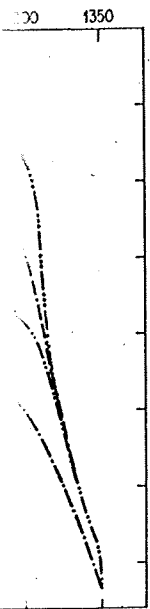
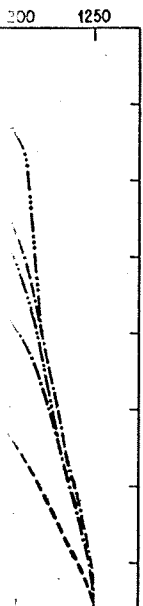


Fig.10D. As Fig.10A. Plate velocity = 8 cm/year.



spreading centre. Plate velocity =



### THERMAL ASPECTS OF SEA-FLOOR SPREADING

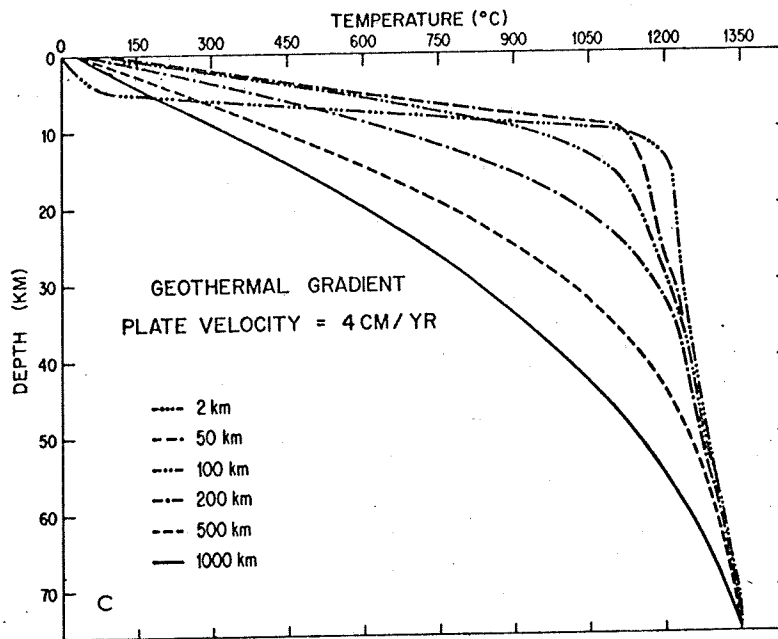


Fig.10C. As Fig.10A. Plate velocity = 4 cm/year.

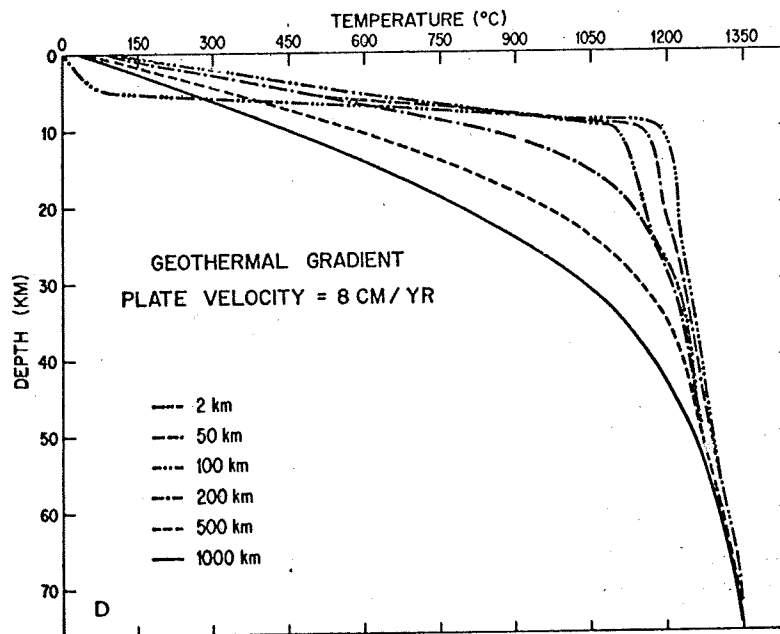


Fig.10D. As Fig.10A. Plate velocity = 8 cm/year.

UNIVERSITY OF UTAH LIBRARY

(1968) on D/H ratios in water vapor from Surtsey Volcano, and the measurements of this ratio in phlogopites of probably deep-seated origin by Sheppard and Epstein (1970), suggest that the delta value for juvenile water should be something like  $-48\%$  with respect to SMOW. From these data Sheppard and Epstein (1970) have concluded that the hydrous minerals in the St. Paul's samples have a contaminated upper-mantle origin. The most likely source of contamination of these samples is ocean water with delta value of  $0\%$  with respect to SMOW. This would mean a 20 – 30% contamination by sea water of these samples. This sea-water contamination will not cause a measurable change in the oxygen-isotopic composition of the samples, because the non-aqueous oxygen in the hydrated phases is about four times more abundant than the aqueous oxygen. Therefore the isotopic evidence confirms the contamination origin of the low-pressure and low-temperature mineral assemblage in the samples from St. Paul's rocks, as was proposed by Melson et al. (1971).

The texture of layer 4a may resemble the classical cumulate texture, as it has been described by Wager et al. (1960). In this case the cumulate texture is not the result of the accumulation of precipitating crystals in a slowly solidifying crystal mush, but is produced by the solidification of a crystal mush formed by partial melting and additional accumulation of liquid phase from below.

#### LAYER 2, OCEAN RIDGE THOLEIITE

The ocean-ridge tholeiites are very uniform in their chemical composition; not only in major components (Engel et al., 1965; Cann, 1971), but also in many trace elements (Kay et al. 1970; Schilling, 1971). The very minor variations these rocks show in their alkali-metal and alkaline earth-metal and rare-earth elements concentrations, can apparently not be correlated with the spreading rate of the ridge they are associated with (Hart, 1971; Schilling, 1971). Schilling (1971) has also concluded that there are no detectable secular variations in the ocean-ridge tholeiites dating from the Cretaceous to the Recent. The amount of tholeiite produced per unit time and per unit length of ridge, seems to be independent of the spreading velocity. This is obvious from the compilation of layer-2 thicknesses for the Pacific and the Atlantic by Ludwig et al. (1970).

Table II is a list of the calculated thickness and composition of layer 2, according to the present model.

TABLE II  
Composition of layer 2

Plate velocity cm/year	Composition of layer 2 as fraction peridotite	Thickness of layer 2 (km)
1	- 0.03	1.2
2	- 0.03	1.3
4	- 0.02	1.3
8	- 0.02	1.5

#### THERMAL ASPECTS OF SEA-FLOOR

The thickness of layer 2 shows... The composition of layer 2 is very... among others, has pointed out that... ridge basalts could indicate only... upper mantle below the ridge crest... beneath the ridge crest never exceeds... respect the model is also in agree...

#### DISCUSSION

The main conclusion of this... may duplicate many of the geo... composition of ocean-ridge thole... demonstrated that besides a late... will also show a vertical chemica... tion on layer 4 should be obvio...

Ocean-ridge heat flow, as cal... facts than in previous models. ... due to latent-heat effects assoc... or 4. This is a conclusion which... done in the course of this work... ridges, and plate thicknesses or... injection of thermal energy at ...

The generation of alkali basa... paper. An inspection of the res... volcanism somewhat off the rid... different from tholeiite. Volcan... this paper, their origin is not d...

Some features of the model... of the upper-mantle zone whic... of the rising current undernea... will start. Changing the dimens... ly affect the amount of tholei... release from the upper mantle... pools underneath the oceanic... width of the rising current und... what the extent of the anomal... layer 3 to  $100^{\circ}\text{C}$  at the ridge... thickness of layer 2.



the measurements of  
 Ward and Epstein (1970),  
 being like - 48% with  
 have concluded that  
 upper-mantle origin.  
 water with delta  
 50% contamination by  
 not cause a measurable  
 cause the non-aqueous  
 ant than the aqueous  
 origin of the low-  
 from St. Paul's rocks,  
 texture, as it has been  
 is not the result of  
 crystal mush, but is pro-  
 melting and additional

composition; not only in  
 many trace elements  
 these rocks show in their  
 concentrations, can apparent-  
 be associated with (Hart,  
 there are no detectable  
 Cretaceous to the Recent.  
 length of ridge, seems to be  
 compilation of layer-2  
 (1970).  
 of layer 2, according to

Thickness of layer 2  
 (km)

1.2  
 1.3  
 1.3  
 1.5

The thickness of layer 2 shows only a very weak dependence on the spreading velocity. The composition of layer 2 is virtually in the center of the basalt range. Schilling (1971), among others, has pointed out that the uniformity of certain trace elements in ocean-ridge basalts could indicate only minor variations in the degree of partial melting in the upper mantle below the ridge crest. In this model the molten fraction in layer 4 underneath the ridge crest never exceeds 8% for any of the spreading velocities. Hence, in this respect the model is also in agreement with the observations.

#### DISCUSSION

The main conclusion of this paper is, that with a fairly simple kinematic model one may duplicate many of the geological aspects of the ocean bottom, notably the constant composition of ocean-ridge tholeiite and the formation of layer 2. Further it has been demonstrated that besides a lateral mineralogical inhomogeneity the suboceanic plate will also show a vertical chemical zonation. The need for more detailed seismic information on layer 4 should be obvious.

Ocean-ridge heat flow, as calculated here, agrees somewhat better with the observed facts than in previous models. The causes for incomplete agreement are unlikely to be due to latent-heat effects associated with phase changes or chemical reactions in layer 3 or 4. This is a conclusion which is based on various numerical experiments which were done in the course of this work. Either plate tectonics, with plate creation at the ocean ridges, and plate thicknesses of about 75 km is wrong, or one should discover a sizable injection of thermal energy at the oceanic ridges into the oceans.

The generation of alkali basalt, near the ridge centre, has not been discussed in this paper. An inspection of the results given in Fig. 6, 7, 8 and 10, should make it clear that volcanism somewhat off the ridge-axis is to be anticipated, the products of which will be different from tholeiite. Volcanic-island tholeiites have not been given any attention in this paper, their origin is not directly comparable to that of ocean-ridge tholeiites.

Some features of the model have been fixed rather arbitrarily. These include the width of the upper-mantle zone which contributes lava for the formation of layer 2, the width of the rising current underneath the oceanic ridges, and the depth at which magma release will start. Changing the dimensions of the source region of ocean-ridge tholeiite will mainly affect the amount of tholeiite to be produced at the ridge centre. If one restricts magma release from the upper mantle to very shallow depth, one will create extensive magma pools underneath the oceanic ridges, for which there exists no evidence. By changing the width of the rising current underneath the ridge from the LVZ, one may manipulate somewhat the extent of the anomalous mantle underneath the ocean ridges. The cooling of layer 3 to 100°C at the ridge centre has little or no influence on the composition and thickness of layer 2.

## APPENDIX 1: COMPUTATIONAL DETAILS

*Initial and boundary conditions and grid spacings*

By means of the finite-difference approximation temperature variations were computed for a sub-oceanic plate from the moment that sea-floor spreading starts until a steady state is reached in a region stretching from the ridge to 1000 km away. The initial temperature distribution in the upper mantle, that is to say before spreading starts, may be obtained as the steady state solution of the heat-conduction equation:

$$\rho C_P \frac{\partial T}{\partial t} = K \frac{\partial^2 T}{\partial z^2} + \rho q \quad (14)$$

Once spreading starts, temperatures are calculated for time intervals of 25,000 years and space intervals of 5 km horizontally and vertically. For the case of an 8 cm/year spreading velocity, the time interval was reduced to 12,500 years. The boundary conditions at the vertical boundaries of the region of interest are the vanishing of horizontal temperature gradients at the plane of symmetry through the ridge centre and at a plane parallel to this at 1500 km away. The upper boundary of the region of interest is the top of layer 3. The temperature at this level may be calculated from a knowledge of the thermal conductivity of layer 2, the thickness of layer 2, the heat flow, and the fact that the top of layer 2 is at 0°C. The temperature at the bottom of the plate is fixed; it is calculated from the steady-state solution of eq. 14 and the observed steady-state heat flow in the ocean basins of 1.30 HFU. This results in a temperature of 1350°C at the bottom of the plate.

*Organisation of the computations*

Eq. 8 and 9 show clearly that the different effects contributing to the variation of the temperature with time may be treated separately; the following sequence was adopted.

- (a) Energy transfer by conduction and radiation.
- (b) Radiogenic heating.
- (c) Latent heat effects.
- (d) Energy transfer by two-phase convection.
- (e) Energy transfer by bulk motion.

*Energy transfer by conduction and radiation; radiogenic heating*

If the temperature field is known at time  $t$ , one may calculate a new temperature at time  $t + \Delta t$ , at point  $(y, z)$ , taking into account effects (a) and (b), by means of the forward finite-difference equation (eq. 15):

$$T(m, n, p + 1) = T(m, n, p) + [G(m, n, p) + q/C_P] \Delta t \quad (15)$$

where:

$$G(m, n, p) = \{ [T(m + 1, n, p) - 2T(m, n, p) + T(m - 1, n, p)] / (\Delta y)^2 + [T(m, n + 1, p) - 2T(m, n, p) + T(m, n - 1, p)] / (\Delta z)^2 + g \alpha [T(m, n, p) - T(m, n + 1, p)] / \Delta z \} K / \rho C_P \quad (16)$$

## THERMAL ASPECTS OF SE

$$y = m\Delta y; \quad z = n\Delta z$$

$m, n,$  and  $p$  are integers.

*Latent-heat effects*

If fusion or solidification

$$T(m, n, p + 1) = T(m, n, p)$$

where:

$$H(m, n, p) = 1 + L / [C_P(\dots)]$$

Eq. 15 is based on eq. 8,  $\partial F / \partial t$  has been replaced by eq. 7.  $K$  is constant, but  $C_P$

The conductive terms in eq. 15 requires that locally the temperature by eq. 1-7, is maintained.

To do this, the bulk composition of the liquid at the previous time step. In all the cases the liquidus temperature and the melted fraction is computed

$$F = (T_N - T_S) / (T_L - T_S)$$

where  $T_N$  is the temperature of the liquid and  $T_S$  is the solidus temperature. Compositions of liquid are

$$X_L = 2(1 + X_A) (T_N - T_S) / (T_L - T_S)$$

$$X_S = (X - F X_L) / (1 - F)$$

where  $X_L$  = composition liquid as fraction peridotite; and  $X_A$

$$X_A = [T_L(z, 0) - T_S(z, 1)] / [T_L(z, 0) - T_S(z, 1)]$$

$$T_{\min} = T_S(z, 0) (X_A + 1)$$

The terms  $T_S(z, 0), T_S(z, 1)$

$$y = m\Delta y; \quad z = n\Delta z; \quad t = p\Delta t$$

$m$ ,  $n$ , and  $p$  are integers.

#### Latent-heat effects

If fusion or solidification occurs, eq. 15 should be changed to eq. 17:

$$T(m, n, p + 1) = T(m, n, p) + [G(m, n, p) + q/C_P] \Delta t / H(m, n, p) \quad (17)$$

where:

$$H(m, n, p) = 1 + L / [C_P(T_L - T_S)] \quad (18)$$

Eq. 15 is based on eq. 8, and eq. 17 and 18 on eq. 9 without the convective terms, in which  $\partial F / \partial t$  has been replaced by eq. 12. Both  $T_L$  and  $T_S$  are pressure- and composition-dependent and may be calculated by linear interpolation, or if required by linear extrapolation, from eq. 3, 4, 5, 6, and 7.  $K$  is constant, but  $C_P = C_P(T)$ .

The conductive terms in eq. 9, which involve the latent heat  $L$ , are taken care of implicitly when one requires that locally the temperature-dependent equilibrium between solid and liquid, as expressed by eq. 1-7, is maintained.

To do this, the bulk composition at point  $(y, z)$  is calculated from the fraction of the liquid phase, the composition of the liquid phase, and the solid composition. These quantities are known from the previous time step. In all these calculations the density difference between solid and liquid is neglected. From the bulk composition and the pressure at point  $(y, z)$  one may calculate from eq. 1-7, the liquidus temperature and the solidus temperature at point  $(y, z)$ . Using eq. 19 a new value for the melted fraction is computed:

$$F = (T_N - T_S) / (T_L - T_S) \quad (19)$$

where  $T_N$  is the temperature which has just been computed.

Compositions of liquid and solid in equilibrium can be calculated from eq. 20 and 21:

$$X_L = 2(1 + X_A) (T_N - T_{\min}) / 2 T_L(z, 1) - X_A \quad (20)$$

$$X_S = (X - F X_L) / (1 - F) \quad (21)$$

where  $X_L$  = composition liquid, expressed as fraction peridotite;  $X_S$  = composition solid, expressed as fraction peridotite; and  $X$  = bulk composition at point  $(y, z)$ .

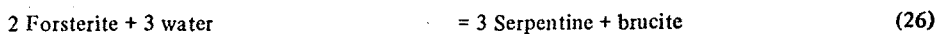
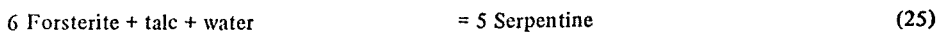
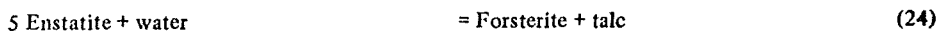
$$X_A = [T_L(z, 0) - T_S(z, 0)] / [T_L(z, 1) - T_S(z, 1) - T_L(z, 0) - T_S(z, 0)] \quad (22)$$

$$T_{\min} = T_S(z, 0) (X_A + 1) - X_A T_S(z, 1) \quad (23)$$

The terms  $T_S(z, 0)$ ,  $T_S(z, 1)$ ,  $T_L(z, 0)$  and  $T_L(z, 1)$  are given by the set of equations 1-7.

### Latent-heat effects of serpentinization

Serpentinization is exothermic. In the model, layer 3 becomes serpentinized according to the reactions:



Kitahara and Kennedy (1967) have given the heats of reaction for (24), (25) and (26), as 16.13, 88.41, and 24.07 kcal., respectively. Though these reactions may perhaps not adequately represent the serpentinization process from a mineralogical point of view, they are probably from a thermal point of view a good approximation. To calculate the amount of heat absorbed or liberated per gram of rock, during serpentinization or deserpentinization, it was assumed that before hydration layer 3 consists of lherzolite, with about 61 wt.% forsterite and 14 wt.% enstatite. Upon hydration, such a rock will contain about 11 wt.% water, which is similar to the amounts of water usually found in oceanic serpentinites. In the calculation it was assumed that the water needed for serpentinization is always available. The average lithostatic pressure in layer 3 is something like 1.5 kbar. An interpolation of the data of Kitahara and Kennedy (1967) indicates that at  $p = 1.5$  kbar, the reactions (24) (25) and (26) have equilibrium temperatures of 680, 510 and 360°C, respectively. In the calculation of the serpentinization effect a check is made after the calculation of  $T_N$  according to eq. 15, whether or not reaction (24) should have occurred. A check is made to what extent the reaction should have advanced, using eq. 27:

$$FR = FR_0 - (T_E - T_N) C_P / \Delta H \quad (27)$$

where  $FR_0$  = degree to which the reaction was completed during the previous time step at point  $(y, z)$ ;  $T_E$  = equilibrium temperature of the reaction; and  $\Delta H$  = latent heat of the reaction per gram of rock.

If  $FR$  is greater than zero, but smaller than unity, the temperature at point  $(y, z)$  should be equal to  $T_E$ . Otherwise one calculates from the rate at which the temperature changes at point  $(y, z)$ ; this can be derived from eq. 15, what fraction from the time step  $\Delta t$  is needed to reach the point at which  $FR = 1$ , in case of serpentinization, or when  $FR = 0$ , in the case of deserpentinization. In other words, it was calculated during what fraction of the time step the temperature at point  $(y, z)$  was equal to  $T_E$ . During the remainder of the time step the temperature is allowed to vary according to eq. 15. After reaction (24) has been investigated in this way, the process is repeated for reactions (25) and (26). At this point effects (a), (b) and (c) have been taken care of.

### Two-phase convection

The liquid velocity due to buoyancy is given by eq. 10, which was derived by Frank (1968) for intergranular movement of the liquid, in a medium consisting of idealized uniform grains. The viscosity of the intergranular liquid is not known: guided by what is known of basalt viscosities (see Bottinga and Weill, 1972) a value of 50 Poise does not seem to be unreasonable. The general observation is that the change in density upon melting of a silicate phase is about 10%, hence the density difference in eq. 10 is estimated to be  $0.3 \text{ cm}^{-3}$ . The experimental work by Spetzler and Anderson (1968) on the elastic properties of the partial melted  $\text{NaCl-H}_2\text{O}$  system, suggests that the melted fraction in the upper mantle is rather small. For the evaluation of  $v_L$  according to eq. 10,  $F$  is taken to be 3%. The dimensions of the grains in the upper mantle may be estimated from the grain sizes observed in ultramafic nodules of deep-seated origin. From the data of White (1966) the mean diameter of the grains in the upper mantle was estimated to be about 3 mm. Using these numbers one arrives at an estimate of

### THERMAL ASPECTS OF SEA-FLOOR

$v_L = 20 \text{ cm/year}$ . Because of uncertainty it is worthwhile to recalculate  $v_L$  for different temperature and composition changes at the surface upward and of the solid phase downward. For cooling or heating, as the case may be, the liquid composition, solid composition, and molten fraction were computed for this point as had been done for effects (a) and (b). A new bulk composition and values for  $T_S$  and  $T_L$  were then calculated. The new  $T_N$  may be calculated from eq. 15:

$$T_N = T_0 / H + (T_S + (T_L - T_S) F_0)$$

where  $T_0$  = temperature at point  $(y, z)$  at the start of eq. 18; and  $F_0$  = molten fraction at the start of eq. 18.

Using eq. 19 a new value for  $F$  may be calculated from eq. 20 and 21. Two-phase convection

### Bulk convection

Bulk convection was taken care of in the calculation of position, and molten fraction, according to eq. 18. As in the case of two-phase convection bulk convection had occurred.

Lastly, basalt extrusion was treated in each space step between 0 and 300 m. If the extrusion of the basalt was accompanied by a change in the bulk composition, again equilibrium values for  $T$ ,  $X_L$ , and  $F$  were calculated for layer 2. In this way the thickness of the

### APPENDIX 2: PHYSICAL CONSTANTS

$\alpha$ : the coefficient of thermal expansion. For basalt  $3.5 \cdot 10^{-5} \text{ deg}^{-1}$  was estimated from the compilation by Kelley (1960), and for the upper mantle  $1.5 \cdot 10^{-5} \text{ deg}^{-1}$ .

$C_P$ : the specific heat at constant pressure. The specific heat is expressed per unit mass. The compilation by Kelley (1960), and for the upper mantle  $1.5 \cdot 10^{-5} \text{ deg}^{-1}$ .

$$C_P = 0.244 + 3.62 \cdot 10^{-5} T - 7.5 \cdot 10^{-8} T^2$$

where  $T$  is the absolute temperature in °K. The pressure-dependence of  $C_P$  is neglected.

$g$ : gravitational acceleration =  $9.8 \text{ m/s}^2$ .

$K$ : thermal conductivity. The measurements for the temperature range 0–1400°C suggest a value of  $0.007 \text{ cal/cm}^2 \text{ deg}^{-1} \text{ cm}^{-1} \text{ s}^{-1}$  for the upper mantle. Fukao (1969) has estimated a thermal conductivity of  $1.5 \times 0.007 \text{ cal/cm}^2 \text{ deg}^{-1} \text{ cm}^{-1} \text{ s}^{-1}$  for ocean-bottom water in this layer. The thermal conductivity of water-filled

$v_L = 20$  cm/year. Because of uncertainty associated with this estimate, it was thought not to be worthwhile to recalculate  $v_L$  for different conditions, hence  $v_L$  was assumed to be constant. Temperature and composition changes at point  $(y, z)$  were computed by translation of the liquid phase upward and of the solid phase downward, at the time intervals required by  $v_L$  and  $v_S$ . Adiabatic cooling or heating, as the case may be, was taken into account. After calculating a new temperature, liquid composition, solid composition, and molten fraction at point  $(y, z)$ , new equilibrium conditions were computed for this point as had been done after the calculation of the temperature change due to effects (a) and (b). A new bulk composition was derived from the values of  $F$ ,  $X_L$ , and  $X_S$ . New values for  $T_S$  and  $T_L$  were then calculated for point  $(y, z)$ . Subsequently a new equilibrium temperature  $T_N$  may be calculated from eq. 28:

$$T_N = T_0/H + (T_S + (T_L - T_S)F_0)(1 - 1/H) \quad (28)$$

where  $T_0$  = temperature at point  $(y, z)$  after the two-phase translation was performed;  $H$  = given by eq. 18; and  $F_0$  = molten fraction at point  $(y, z)$  after two-phase translation was performed.

Using eq. 19 a new value for  $F$  may be computed. And new values for  $X_L$  and  $X_S$  may be calculated from eq. 20 and 21. Two-phase convection was supposed to occur only below layer 3.

#### Bulk convection

Bulk convection was taken care of by performing translations of temperature, liquid and solid composition, and molten fraction, according to the chosen plate-velocity field on Fig. 1; adiabatic corrections were applied. As in the case of two-phase convection, chemical equilibrium was established after bulk convection had occurred.

Lastly, basalt extrusion was treated, by letting escape to the surface 0.3 of a liquid fraction present in each space step between 0 and 30 km depth, underneath the ridge center during each time step. The extrusion of the basalt was accompanied by a compensatory settling of the overlying solid phases. Again equilibrium values for  $T$ ,  $X_L$ ,  $X_S$  and  $F$  were calculated. The extruded basalt was used to build up layer 2. In this way the thickness and composition of layer 2 could be derived.

#### APPENDIX 2: PHYSICAL CONSTANTS

$\alpha$ : the coefficient of thermal expansion. Using the compilation of Skinner (1966); a value of  $3.5 \cdot 10^{-5} \text{ deg}^{-1}$  was estimated for the thermal expansion of an assemblage of pyroxene and olivine.

$C_p$ : the specific heat at constant pressure. This quantity is strongly temperature-dependent. When the specific heat is expressed per unit of mass, most silicate minerals have similar specific heats. From the compilation by Kelley (1960), the specific-heat formula for diopside was recalculated to:

$$C_p = 0.244 + 3.62 \cdot 10^{-5} T - 7.27 \cdot 10^3/T^2 \text{ cal.g}^{-1} \text{ deg}^{-1}$$

where  $T$  is the absolute temperature. This expression was used in all the computations of this paper.

The pressure-dependence of  $C_p$  is not known.

$g$ : gravitational acceleration =  $980.6 \text{ cm/sec}^2$ .

$K$ : thermal conductivity. The measurements of Kawada (1966) on ultramafic rocks, in the temperature range  $0-1400^\circ\text{C}$  suggest a value of  $0.007 \text{ cal. sec}^{-1} \cdot \text{cm}^{-1} \cdot \text{deg}^{-1}$  for the thermal conductivity of the upper mantle. Fukao (1969) has concluded from his measurements on olivine that the thermal conductivity under upper-mantle pressure and -temperature of this mineral is constant. For layer 2 a thermal conductivity of  $1.5 \times 0.007 \text{ cal. sec}^{-1} \text{ cm}^{-1} \text{ deg}^{-1}$  was taken, because of the presence of ocean-bottom water in this layer. The factor 1.5 was suggested by the work of Cermak (1967) on the thermal conductivity of water-filled sediments.

$L$ : latent heat of fusion. This quantity is not known for rocks. A value of 100 cal/g was selected, this value is close to the centre of the range in which all values for silicate minerals listed by Robie and Waldbaum (1968) fall.

$q$ : radiogenic heat generation in the upper mantle. Tatsumoto et al. (1965) have reported the Th, U, K, and Rb concentrations in oceanic tholeiites. These elements will be concentrated in the low-melting fraction upon partial fusion in the upper mantle. Therefore  $q$  for a pyrolytic upper mantle should be about  $4.9 \cdot 10^{-15}$  cal.g<sup>-1</sup> sec<sup>-1</sup>.

$\rho$ : the density of layer 4, was taken to be 3.3 g/cm<sup>3</sup> on the average (Wang, 1970).

## REFERENCES

- Anderson, D.L. and Sammis, C., 1970. Partial melting in the upper mantle. *Phys. Earth Planet. Inter.*, 3: 41-50.
- Arnason, B. and Sigurgeirson, T., 1968. Deuterium content of water vapor and hydrogen in volcanic gas at Surtsey, Iceland. *Geochim. Cosmochim. Acta*, 32: 807-813.
- Bottinga, Y., 1972. Thermal aspects of sea-floor spreading. *Trans. Am. Geophys. Union*, 53: 537 (abstract).
- Bottinga, Y. and Allegre, C.J., 1973. Thermal aspects of sea-floor spreading and the nature of the oceanic crust. *Tectonophysics*, 18: 1-17.
- Bottinga, Y. and Weill, D.F., 1972. The viscosity of magmatic silicate liquids: A model for calculation. *Am. J. Sci.*, 272: 438-475.
- Cann, J.R., 1971. Major element variations in ocean-floor basalts. *Philos. Trans. R. Soc. London, Ser. A*, 268: 495-506.
- Cermak, V., 1967. Coefficient of thermal conductivity of some sediments, its dependence on density and on water content of rocks. *Chem. Erde*, 26: 271-278.
- Cohen, L.H., Ito, K. and Kennedy, G.C., 1967. Melting and phase relations in an anhydrous basalt to 40 kb. *Am. J. Sci.*, 265: 475-518.
- Craig, H., 1961. Standards for reporting concentrations of deuterium and oxygen-18 in natural waters. *Science*, 133: 1833-1834.
- Engel, A.E.J., Engel, C.G. and Havens, R.G., 1965. Chemical characteristics of oceanic basalts and the upper mantle. *Geol. Soc. Am. Bull.*, 76: 719-734.
- Frank, F.C., 1968. Two-component flow model for convection in the earth's upper mantle. *Nature*, 220: 350-352.
- Frey, F.A., 1970. Rare-earth and potassium abundances in St. Paul's rocks. *Earth Planet. Sci. Lett.*, 7: 351-360.
- Fukao, Y., 1969. On radiative heat transfer and thermal conductivity in the upper mantle. *Bull. Earthquake Res. Inst., Tokyo Univ.*, 47: 549-569.
- Green, D.H., 1971. Composition of basaltic magmas as indicators of origin: application to oceanic volcanism. *Philos. Trans. R. Soc. London, Ser. A*, 268: 707-725.
- Green, D.H. and Ringwood, A.E., 1967. The genesis of basaltic magma. *Contrib. Mineral. Petrol.*, 16: 103-190.
- Harrison, C.G.A., 1968. Formation of magnetic anomaly patterns by dike injection. *J. Geophys. Res.*, 73: 2137-2142.
- Hart, S.R., 1971. K, Rb, Cs, Sr, and Ba contents and Sr isotope ratios of ocean-floor basalts. *Philos. Trans. R. Soc. London, Ser. A*, 268: 573-588.
- Horai, K., Chessman, M. and Simmons, G., 1970. Heat flow measurements on the Reykjanes ridge. *Nature*, 225: 264-265.
- Ito, K. and Kennedy, G.C., 1967. Melting and phase relations in a natural peridotite to 40 kbar. *Am. J. Sci.*, 265: 211-217.
- Ito, K. and Kennedy, G.C., 1968. Melting and phase relations in the plane tholeiite-ilmenite-nepheline basalt to 40 kbar with geological implications. *Contrib. Mineral. Petrol.*, 19: 177-211.
- Kawada, K., 1966. Studies of the thermal state of the earth, 17. Variation of thermal conductivity of rocks, 2. *Bull. Earthquake Res. Inst., Tokyo Univ.*, 44: 1071-1091.
- Kay, R., Hubbard, N.J. and Gast, P.W., 1967. Volcanic rocks. *J. Geophys. Res.*, 72: 5321-5355.
- Kelley, K.K., 1960. *Contributions to the Content, Heat Capacity, and Entropy of the Earth's Crust*. Government Printing Office, Washington.
- Kitahara, S. and Kennedy, G.C., 1967. Melting and phase relations in the system MgO-SiO<sub>2</sub>-H<sub>2</sub>O at pressures to 40 kb. *J. Geophys. Res.*, 71: 5321-5355.
- Langseth Jr., M.G., Le Pichon, X. and Le Pichon, X., 1969. Models and structures of the oceanic crust. *Sea*, Wiley, New York, N.Y., 4 (1): 1-10.
- Lister, C.R.B., 1972. On the thermal structure of the oceanic crust. *Sea*, Wiley, New York, N.Y., 4 (1): 11-20.
- Ludwig, W.J., Hafe, J.E. and Drake, C., 1967. *Sea*, Wiley, New York, N.Y., 4 (1): 21-30.
- Matthews, D.H. and Bath, J., 1967. *Sea*, Wiley, New York, N.Y., 4 (1): 31-40.
- Melson, W.G., Jarosewich, E., Bowen, D.R., Hart, S.R. and Thompson, T.B., 1969. A high temperature mantle derived from radiometric ages, and implications. *Unpublished*.
- Moore, J.G., 1970. Water content of the oceanic crust. *Sea*, Wiley, New York, N.Y., 4 (1): 21-30.
- Peck, D.L., Wright, T.L. and Moore, J.G., 1970. *Hawaii, Bull. Volcanol.*, 29: 629-640.
- Press, F., 1970. Earth models consistent with seismic data. *Sea*, Wiley, New York, N.Y., 4 (1): 41-50.
- Richter, D.H. and Moore, J.G., 1966. *Prof. Pap.*, 537-B: B1-B26.
- Ringwood, A.E., 1966. *Mineralogy of the Earth's Crust*. M.I.T. Press, Cambridge, Mass., pp. 1-100.
- Robie, R.A. and Waldbaum, D.R., 1968. *Mineralogical Data*. U.S. Government Printing Office, Washington.
- Schilling, J.G., 1971. Sea-floor evolution. *Sea*, Wiley, New York, N.Y., 4 (1): 51-60.
- Sclater, J.G. and Francheteau, J., 1970. Tectonic and geochemical models for the oceanic crust. *Sea*, Wiley, New York, N.Y., 4 (1): 61-70.
- Sheppard, S.M. and Epstein, S., 1970. Crustal origin. *Earth Planet. Sci. Lett.*, 7: 361-370.
- Skinner, B.J., 1966. Thermal expansion of rocks. *Contrib. Mineral. Petrol.*, 16: 191-200.
- Spetzler, H. and Anderson, D.L., 1967. Attenuation in a simple binary system. *J. Geophys. Res.*, 72: 473-482.
- Talwani, M., Windish, C.C. and Langseth Jr., M.G., 1967. *J. Geophys. Res.*, 72: 473-482.
- Tatsumoto, M., Hedge, C.E. and Engel, A.E.J., 1965. The ratio strontium-87/strontium-86 and the ratio strontium-87/strontium-86. *J. Geophys. Res.*, 70: 19-27.
- Vine, F.J. and Matthews, D.H., 1963. *Sea*, Wiley, New York, N.Y., 4 (1): 1-10.
- Von Herzen, R. and Simmons, G., 1967. *Sea*, Wiley, New York, N.Y., 4 (1): 11-20.
- Wager, L.R., Brown, M.G. and Wadsworth, W.J., 1967. *Sea*, Wiley, New York, N.Y., 4 (1): 21-30.
- Wang, C., 1970. Density and constant pressure thermal conductivity of the upper mantle. *Sea*, Wiley, New York, N.Y., 4 (1): 31-40.
- Wenner, D.B. and Taylor Jr, H.P., 1967. *Sea*, Wiley, New York, N.Y., 4 (1): 41-50.

- Kay, R., Hubbard, N.J. and Gast, P.W., 1970. Chemical characteristics and origin of oceanic ridge volcanic rocks. *J. Geophys. Res.*, 75: 1585-1613.
- Kelley, K.K., 1960. *Contributions to the Data on Theoretical Metallurgy, XIII. High Temperature Heat Content, Heat Capacity, and Entropy Data for the Elements and Inorganic Compounds*. U.S. Government Printing Office, Washington D.C.
- Kitahara, S. and Kennedy, G.C., 1967. The calculated equilibrium curves for some reactions in the system  $MgO-SiO_2-H_2O$  at pressures up to 30 kbar. *Am. J. Sci.*, 265: 211-217.
- Langseth Jr., M.G., Le Pichon, X. and Ewing, M., 1966. Crustal structure of the mid-ocean ridges. *J. Geophys. Res.*, 71: 5321-5355.
- Le Pichon, X., 1969. Models and structure of the oceanic crust. *Tectonophysics*, 7: 385-401.
- Lister, C.R.B., 1972. On the thermal balance of a mid-ocean ridge. *Geophys. J.*, 26: 515-535.
- Ludwig, W.J., Hafe, J.E. and Drake, C.L., 1970. Seismic refraction. In: A.E. Maxwell (Editor), *The Sea*. Wiley, New York, N.Y., 4 (1): 53-84.
- Matthews, D.H. and Bath, J., 1967. Formation of magnetic anomaly pattern of Mid-Atlantic Ridge. *Geophys. J.*, 13: 349-357.
- Melson, W.G., Jarosewich, E., Bowen, V.T. and Thompson, G., 1967. St. Peter and St. Paul rocks: A high temperature mantle derived intrusion. *Science*, 155: 1532-1535.
- Melson, W.G., Hart, S.R. and Thompson, G., 1971. St. Paul's rocks, equatorial Atlantic: Petrogenesis, radiometric ages, and implications on sea-floor spreading. *Woods Hole Oceanogr. Inst. Ref.*, 71-20. unpublished.
- Moore, J.G., 1970. Water content of basalts erupted on the ocean floor. *Contrib. Mineral. Petrol.*, 28: 272-279.
- Peck, D.L., Wright, T.L. and Moore, J.G., 1966. Crystallization of tholeiitic basalt in Alea Lava Lake. *Hawaii, Bull. Volcanol.*, 29: 629-655.
- Press, F., 1970. Earth models consistent with geophysical data. *Phys. Earth Planet. Inter.*, 3: 3-22.
- Richter, D.H. and Moore, J.G., 1966. Petrology of the Kilauea Ika Lava Lake, Hawaii. *U.S. Geol. Surv. Prof. Pap.*, 537-B: B1-B26.
- Ringwood, A.E., 1966. Mineralogy of the mantle. In: P.M. Hurley (Editor), *Advances in Earth Science*. M.I.T. Press, Cambridge, Mass., pp. 357-399.
- Robie, R.A. and Waldbaum, D.R., 1968. *Thermodynamic Properties of Minerals and Related Substances at 298.15°K (25.0°C) and One Atmosphere (1.013 bars) Pressure and at Higher Temperatures*. U.S. Government Printing Office, Washington D.C.
- Schilling, J.G., 1971. Sea-floor evolution: Rare-earth evidence. *Philos. Trans. R. Soc. London, Ser. A*, 268: 663-706.
- Slater, J.G. and Francheteau, J., 1970. The implications of terrestrial heat-flow observations on current tectonic and geochemical models of the crust and upper mantle. *Geophys. J.*, 20: 509-542.
- Sheppard, S.M. and Epstein, S., 1970. D/H and  $^{18}O/^{16}O$  ratios of minerals of possible mantle or lower crustal origin. *Earth Planet. Sci. Lett.*, 9: 232-239.
- Skinner, B.J., 1966. Thermal expansion. *Geol. Soc. Am., Mem.*, 97: 75-96.
- Spetzler, H. and Anderson, D.L., 1968. The effect of temperature and partial melting on velocity and attenuation in a simple binary system. *J. Geophys. Res.*, 73: 6051-6060.
- Talwani, M., Windish, C.C. and Langseth Jr., M.G., 1971. Reykjanes ridge crest: A detailed geophysical study. *J. Geophys. Res.*, 76: 473-517.
- Tatsumoto M., Hedge, C.E. and Engel, A.E.J., 1965. Potassium, rubidium, strontium, thorium, uranium, and the ratio strontium-87/strontium-86 in oceanic tholeiitic basalt. *Science*, 150: 886-888.
- Vine, F.J. and Matthews, D.H., 1963. Magnetic anomalies over oceanic ridges. *Nature*, 199: 947-949.
- Von Herzen, R. and Simmons, G., 1972. Two heat-flow profiles across the Atlantic ocean. *Earth Planet. Sci. Lett.*, 15: 19-27.
- Wager, L.R., Brown, M.G. and Wadsworth, W.J., 1960. Types of igneous cumulates. *J. Petrol.*, 1: 73-85.
- Wang, C., 1970. Density and constitution of the mantle. *J. Geophys. Res.*, 75: 3264-3284.
- Wenner, D.B. and Taylor Jr, H.P., 1971. Temperatures of serpentinization of ultramafic rocks based on  $O^{18}/O^{16}$  fractionation between coexisting serpentine and magnetite. *Contrib. Mineral. Petrol.*, 32: 165-285.

- White, R.W., 1966. Ultramafic inclusions in basaltic rocks from Hawaii. *Contrib. Mineral. Petrol.*, 12: 245-314.
- Wright, T.L. and Weiblen, P.W., 1968. Mineral composition and paragenesis in tholeiitic basalt from Makaopuhi Lava Lake, Hawaii. *Geol. Soc. Am., Spec. Pap.*, 115: 242-242 (abstract).
- Wyllie, P.J., 1971. Role of water in magma generation and initiation of diapiric uprise in the mantle. *J. Geophys. Res.*, 76: 328-338.
- Yoder Jr., H.S. and Kushiro, I., 1969. Melting of a hydrous phase: phlogopite. *Am. J. Sci.*, 267 (A): 558-582.

## ULTRASONIC PULSE VE

M.T. GLADWIN and F.D. STACEY

*Physics Department, University of C*

(Accepted for publication June 14.

## ABSTRACT

Gladwin, M.T. and Stacey, F.D., 19  
*physics*, 21: 39-45.

A method of measuring with nan-  
tances of a few metres in rock in str-  
pulses repeated at intervals of 20 m-  
situation the measurements are sens-  
has been used to seek changes in str-  
thermal stresses were clearly seen. c-  
tunnel is implied.

## INTRODUCTION

As part of a survey of possi-  
referred to evidence that travel  
tion paths included the focal v-  
experiment to measure travel t-  
range 200 - 300 km. The plat-  
immediately obvious. In most  
increases in elastic-wave veloci-  
higher pressures pore closure c-  
tends toward the much smaller  
superposition of axial compres-  
similar to those produced by c-  
et al., 1963), and although the  
to deviatoric stresses also decre-  
that seismic velocities can be s-  
in the earth, i.e., within the up-  
visaged by Tsuboi et al. (1962  
plosion or recording sites. Att-  
ported (Kanamori, 1970; Fed-  
Eisler, 1967, 1969) appear ma-